Sustainable Food Technology

ROYAL SOCIETY OF CHEMISTRY

PAPER

View Article Online
View Journal

Cite this: DOI: 10.1039/d5fb00825e

Antimicrobial silver nanoparticle-doped poly(vinyl alcohol)/guar gum/gum ghatti nanocomposites: a multifaceted step towards sustainable packaging

Veena G. Bhat,[a] Saraswati P. Masti, *[a] Shivayogi S. Narasagoudr,[b] Lingaraj Kariyappa Kurabetta,[a] Manjushree Nagaraj Gunaki,[a] Ajitkumar Appayya Hunashyal,[a] Ravindra B. Chougale[c] and Ravindra B. Malabadi[de]

The present study describes the green synthesis of silver nanoparticles (AgNPs) using a fixed concentration of poly(vinyl alcohol) (PVA)/guar gum (GG)/gum ghatti (GGh) blend solution with different concentrations of $AgNO_3$ solution at room temperature and fabrication of PVA/GG/GGh/AgNP nanocomposites (PGGA) using a simple solvent casting method. The effect of the inclusion of AgNPs on the surface morphology, mechanical and thermal properties of the obtained PGGA nanocomposites was studied using Scanning Electron Microscopy (SEM), Fourier Transform Infrared (FTIR) spectroscopy, a Universal Testing Machine (UTM), Thermogravimetric Analysis (TGA) and Differential Scanning Calorimetry (DSC), respectively. Also, the results were compared with the blend film PVA/GG/GGh (PGGA-0) without AgNPs. The X-ray diffraction (XRD) study confirmed the formation of AgNPs (17–40 nm), and SEM analysis suggested homogeneous distribution of AgNPs in the polymer matrix. The presence of AgNPs does not change the position of IR peaks in PGGA nanocomposites. There was improvement in the hydrophobicity (63.6 ± 3.3° to 96.3 ± 2.5°) and thermal stability of PGGA nanocomposites compared to the PGGA-0 blend film. Further analysis of the results suggested an increase in the elongation at break of PGGA-4 nanocomposites with an increase in the concentration of AgNPs (0.2% w/v). Moisture adsorption was significantly decreased by the addition of AgNPs into the polymer matrix compared to the PGGA-0 blend film. The increase in AgNP content effectively inhibited the growth of bacteria. The soil burial test indicated biodegradation of the PGGA nanocomposites. Application studies on fresh coriander leaves confirmed that PGGA-1 films effectively enhanced shelf life and quality retention under ambient conditions. Improved moisture control, chlorophyll preservation, and sensory attributes highlight their practical potential in sustainable food packaging.

Received 31st October 2025
Accepted 24th March 2026

DOI: 10.1039/d5fb00825e

rsc.li/susfoodtech

1. Introduction

Nanomaterials are in the limelight due to their size-dependent properties compared to bulk materials.[1] At present, nanoparticles are extensively synthesized and utilized owing to their diverse and versatile applications. The presence of a large surface area with tunable size and properties makes them prospective candidates for a wide spectrum of applications such as drug delivery, pharmaceuticals, food packaging and biotechnology.[2] Various nanomaterials such as zinc oxide (ZnO), titanium dioxide (TiO_2), copper (Cu), silver (Ag) and gold (Au) grabbed the interest in recent years.[3] Among all, AgNPs, due to their unique physicochemical properties and chemical inertness, find applications in various fields such as food additives, packaging and the biomedical field.[4] Traditionally, AgNPs offer good broad-spectrum antimicrobial properties over a wide range of microorganisms. Moreover, this inherent antimicrobial efficacy of AgNPs, even at low concentrations, was employed to design many biomedical products.[5,6] Das *et al.* studied the antioxidant properties of AgNPs and thus are beneficial in scavenging free radicals produced in the human body.[7] Hence, many medicinal and anti-ageing formulations with AgNPs prove to be effective in minimizing side effects caused by the generation of free radicals. Also, studies on the incorporation of plant extracts such as aloe vera plant extract and boswellic acid in polymer blends have improved antimicrobial properties.[8,9] However, the use of nanoparticles is a far more effective and commercially viable technique to enhance antimicrobial properties.[7] Therefore, different synthetic

[a]Department of Chemistry, Karnatak Science College, Dharwad-580 001, Karnataka, India. E-mail: dr.saraswatimasti@yahoo.com
[b]Reliance Industries Limited, Mumbai- 400 021, Maharashtra, India
[c]P.G. Department of Studies in Chemistry, Karnatak University, Dharwad-580 003, Karnataka, India
[d]Miller Blvd, NW, Edmonton, AB, Canada
[e]Department of Applied Botany, Mangalore University, Mangalagangotri-574 199, Mangalore, Karnataka, India

methods such as chemical, photochemical, thermal and electrochemical methods were used in the preparation of AgNPs.[10] Among the reducing agents, silver nanoparticles synthesized using sodium borohydride, hydrazine, ethylene glycol, *etc.*, may be associated with toxic chemicals and hence find limited applications.[11] To minimize chemical wastage during the synthesis and to reduce the extra cost of chemical reagents, green synthesis was employed. The reducing and protecting ability of the polymers has been advantageous in the green and cost-effective synthesis of AgNPs.[2] Also, *in situ* generation of AgNPs using polymer helps in two ways: adsorption to the surface of NPs causes repulsion between NPs, and an increase in viscosity slows down the accumulation of AgNPs. Thus, they are convenient to use for the synthesis of AgNPs.[2,12] Currently, polysaccharide-based hybrid materials containing AgNPs are receiving increasing attention, as they are found to impart better mechanical and functional properties. In these nanocomposites, polymers were used as stabilizers for the production of nanoparticles and as a supporting matrix for the incorporation of nanoparticles.[13] The presence of abundant hydroxyl groups acts as reducing and capping agents for the generation of NPs from aqueous solution.[12] In this context, safer precursors such as PVA, GG, GGh, *etc.*, have gained much importance as an alternative to chemical reducing agents for the synthesis of AgNPs.[14,15] Hence, our research work is focused on the *in situ* preparation of AgNPs using GG, GGh and PVA blend solution.[7] The carbonyl, hydroxyl and amino groups present in the polymers reduce the silver ions.[16,17]

Natural gums are biopolymers that find multifaceted applications in food, pharmaceuticals and drug delivery. Beneficial aspects such as nontoxicity, biodegradability, stability and physicochemical properties make them prospective candidates for packaging applications.[18] Also, they act as suitable reagents for the *in situ* synthesis of silver nanoparticles. Gums such as cashew gum, tragacanth gum, gum acacia, *etc.*, were used in the synthesis of AgNPs.[19,20] Gum ghatti (GGh) is yet another naturally occurring complex polysaccharide obtained from the bark of *Anogeissus latifolia*.[21] Gum ghatti-based blend films and hydrogels find application in different fields such as the food industry and medicine.[22] These favourable properties make GGh suitable for the synthesis of AgNPs owing to the presence of abundant –OH groups.[23] The study conducted by Palem *et al.* showed the green synthesis of AgNPs from guar gum solution.[24]

Guar gum (GG), a water-soluble polysaccharide (galactomannan) obtained from cluster beans, is one of the biopolymers with high molecular weight and is easily available.[5,25] GG finds extensive use on account of its biodegradability and biocompatibility.[26] The ability to form a highly viscous solution in water finds application in the field of the food and dairy industry.[27] Its film-forming ability and formation of hydrogen bonding with other polymers make it a suitable candidate for pharmaceuticals, textiles, printing and biomedical applications.[1,28] These properties make it convenient for blending with PVA to tailor the physicochemical properties of the blend films.[29] Polysaccharide-based films are usually brittle in nature. To overcome the brittleness, glycerol is used as a plasticiser,[6] as it can form hydrogen bonds with hydroxyl groups of the polymer backbone, thus bringing about compatibility and improving the mechanical properties of the end product.[30]

PVA is one of the synthetic, water-soluble and biodegradable polymers, extensively used as a host polymer for the incorporation of AgNPs.[31,32] Its biocompatible nature and better film-forming ability are favourable for blending with other biopolymers such as CS, starch, GG, GGh, *etc.*[33] The properties such as chemical inertness, adequate film-forming ability[34] and mechanical strength[35] make it suitable for biomedical applications[36] and food packaging.[37,38] The ability of PVA to form hydrogen bonds with other polymers was exploited to improve the performance of the film.[39] The poor antimicrobial properties of PVA, GG and GGh can be improved by the incorporation of AgNPs in the nanocomposites.

Since few studies have been carried out on the nanocomposites containing GG, GGh and AgNPs due to the formation of brittle films,[73–75] our attempt involves the development of novel eco-friendly nanocomposites containing a fixed ratio of GG, GGh and PVA with different weight percentages of *in situ* generated AgNPs using an environmentally benign solvent casting technique.[76–78] The influence of AGNPs on the structural and physical properties of the PGGA nanocomposites was evaluated using different analytical techniques. Also, the prepared PGGA nanocomposites were studied by soil burial test and antibacterial activity against *S. aureus* and *E. coli* bacteria to find possible applications in food packaging.[79–81]

2. Experimental section

2.1. Materials

Poly(vinyl alcohol) with $M_w \approx 125\,000$ and 85–89% degree of hydrolysis, guar gum and gum ghatti were procured from Loba Chemie Pvt. Ltd, Mumbai. $AgNO_3$ and glycerol were procured from Himedia. All the solutions were prepared using double-distilled water.

2.2. Preparation of silver nanoparticle-incorporated nanocomposites

The nanocomposites of PVA/guar gum/gum ghatti and *in situ* generated AgNPs were prepared by using a fixed concentration of PVA, GG and GGh with varying concentrations of $AgNO_3$. Briefly, PVA (1.8% w/v) solution was prepared in distilled water and agitated on a magnetic stirrer at 80 °C for 4 h. Meanwhile, 0.1% (w/v) GG and 0.1% (w/v) GGh solutions were prepared in distilled water separately and stirred on a magnetic stirrer until the solution becomes homogeneous. A series of blend solutions with fixed concentration of PVA, GG and GGh were mixed with different concentrations of $AgNO_3$ (0.05, 0.1, 0.15, and 0.2% w/v) solution. The resultant blend solutions were stirred on a magnetic stirrer for 4 h. The colour change during this stage indicates the reduction of silver ions to AgNPs. Then sonicated for 10 min and transferred to a Petri dish. The films were dried at room temperature (27 ± 2 °C) for 72 h. After drying, the films were removed from the Petri dishes, preserved in airtight bags,

Table 1 Composition of the PVA/guar gum/gum ghatti/AgNP nanocomposites

Sample code	Poly(vinyl alcohol) (%)	Guar gum (%)	Gum ghatti (%)	1% glycerol (mL)	$AgNO_3$ (%)
PGGA-0	1.8	0.1	0.1	10	—
PGGA-1	1.8	0.1	0.1	10	0.05
PGGA-2	1.8	0.1	0.1	10	0.10
PGGA-3	1.8	0.1	0.1	10	0.15
PGGA-4	1.8	0.1	0.1	10	0.20

and used for characterization. The composition of nanocomposites is given in Table 1.[82,83]

3. Characterization techniques

3.1. Mechanical properties

The thickness of the nanocomposites was recorded with a manual digital micrometre with 0.001 mm resolution (thickness measurement gauge, Mitutoyo high accuracy micrometre-S700, Japan). Each film of size 25 mm × 100 mm was taken, and the thickness was measured at five different positions of the film. The tensile strength (TS) and elongation at break (EB) of the nanocomposites were measured using a universal testing machine according to the ASTM-D882-1992 standard (Dak system INC, Gen-NXT series 7200-1KN, Mumbai, India). The rectangular film of size 25 mm × 100 mm was fixed between metallic grips, which were separated by a distance of 50 mm. A 1 KN load cell was used, and the upper grip was moved at a speed of 1 mm min^{-1}. Three trials were taken for each film sample at room temperature, and the average was considered for studying the mechanical properties.

3.2. Scanning electron microscopy (SEM)

The morphology of the AgNPs and nanocomposites was studied using a JEOL In Touch Scope (JEOL In Touch Scope, JSM-IT500, Tokyo, Japan) scanning electron microscope. The film samples were coated with gold by sputtering and mounted on a metal stub before scanning. An accelerating voltage of 10 kV was used to scan the samples.[84]

3.3. Fourier transform infrared (FTIR) spectroscopy

The structural changes that occurred due to interactions among the polymers and AgNPs were analyzed using FTIR spectroscopy (PerkinElmer Spectrum Version 10.5.4 spectrometer, Shelton, USA) in the wavelength range of 4000 cm^{-1} to 400 cm^{-1}.

3.4. Water contact angle (WCA) measurement

The hydrophilic/hydrophobic nature of the film was studied by water contact angle measurement (Format Version:3.6, KYOWA Interface Measurement and Analysis System (FAMAS), Japan). A water droplet was placed using a syringe on the surface of the film, and the images of the droplets were captured using a high resolution camera. All the measurements were carried out at room temperature. The size of the water drop was kept constant while recording the contact angle. The average value of the three measurements was considered for the interpretation of the results.[85,86]

3.5. Thermogravimetric analysis (TGA)

A thermal analyzer SDT Q600 V20.9 Build 20 (TA Instruments, New Castle, Delaware, USA) was used to study the thermal degradation behaviour of the nanocomposites. About 4–5 mg of the sample was taken and heated at a rate of 10 °C min^{-1} under a nitrogen atmosphere with a flow rate of 50 mL min^{-1}. The analysis was performed from room temperature to 600 °C.

3.6. Differential scanning calorimetry (DSC)

The thermal properties during the phase transition and associated enthalpy changes were studied using differential scanning calorimetry (DSC Q20-V24.4 Build 116, TA instruments, Walters LLC, New Castle, Delaware, USA). 1–2 mg of the sample was taken and heated from a temperature of 25 °C to 400 °C under a nitrogen atmosphere (flow rate 50 mL min^{-1}) at a heating rate of 10 °C.

3.7. X-ray diffraction (XRD) analysis

The crystalline nature of nanocomposites and AgNPs was evaluated using X-ray diffractograms recorded with an X-ray diffractometer (powder), Model: SmartLab SE, Rigaku Tokyo, Japan. The X-ray beam was obtained from a copper target (Cu Kα, $\lambda = 1.5418$ Å) source at a voltage of 30 kV and 20 mA. The XRD patterns were recorded for each sample in the range $2\theta = 10°$ to 70° at a scan speed of 2° min^{-1}. The AgNP size was calculated using the Debye–Scherrer formula (1) (ref. 40):

$$d = \frac{K\lambda}{\beta \cos\theta} \quad (1)$$

where d is the average particle size, β is the line broadening, θ is the Bragg's angle, λ is the X-ray wavelength and K is the dimensionless shape factor.

3.8. Moisture adsorption (MA)

The moisture adsorption was determined by considering equilibrium moisture adsorption with respect to the mass of the dry sample. The samples with a size of 20 mm × 20 mm were taken and dried in an oven at 100 °C for 24 h. The dry mass was recorded.[41] The films were kept in the open atmosphere for 24 h, and the mass was noted. All the weights were recorded with a digital weighing balance having an accuracy of 0.0001 g. The

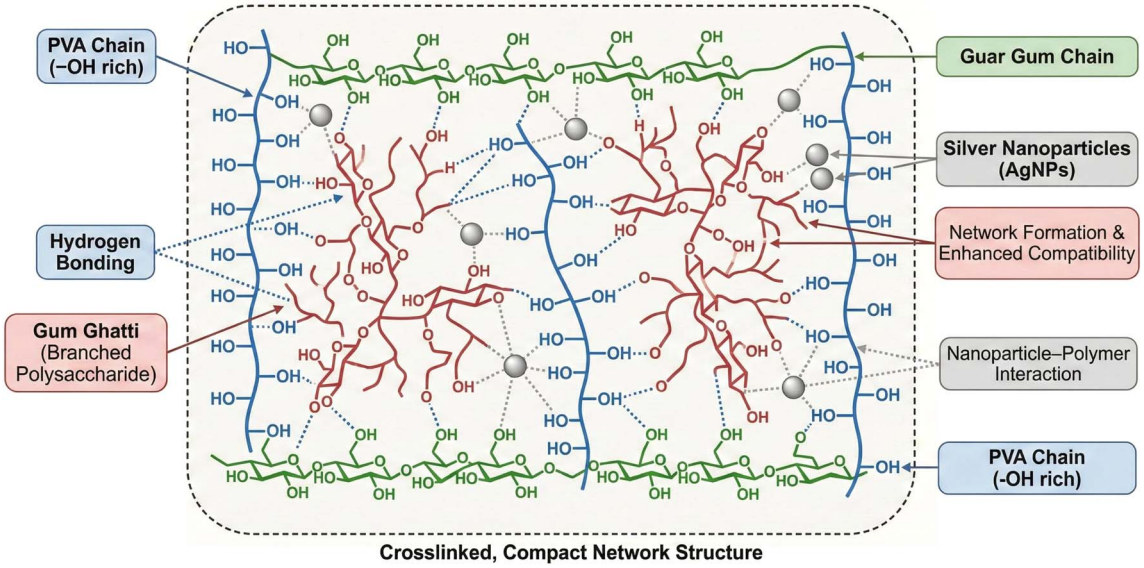

Scheme 1 Schematic diagram illustrating the possible interactions between PVA/GG/GGh and AgNPs.

analysis of moisture adsorption was performed in triplicate, and the MA of the individual film was calculated using eqn (2).

$$\text{Moisture adsorption } (\%) = \frac{(W_2 - W_1)}{W_1} \times 100 \qquad (2)$$

where W_1 (g) is the initial mass of the dry film and W_2 (g) is the mass of the film after moisture adsorption.

3.9. Antibacterial properties

The agar well diffusion method was used to analyse antibacterial properties against Gram-negative bacteria *(Escherichia coli)* and Gram-positive bacteria *(Staphylococcus aureus)*.[11] The bacterial culture was grown overnight in the culture medium and incubated at 37 °C. Nutrient agar medium (pH 7) was prepared in a conical flask and sterilized at a pressure of 15 lbs for 30 min. The sterilized agar medium was poured into Petri plates inside a laminar airflow chamber and allowed to solidify. The bacterial culture was spread evenly on the solid media using an L-shaped spreader. After a few minutes, the nanocomposite solution (10 mg ml^{-1}) was added into the hole made at the centre. All the Petri plates were labelled and kept in an incubator for the development of culture for 24 h at 37 °C. After the incubation period, the diameter of the zone of inhibition was measured in millimetres.

3.10. Soil burial test

It is one of the prime concerns that packaging materials, after their use, must degrade under environmental conditions. Also, the waste produced should not harm the living organisms. The films made of biodegradable polymers are mainly rich in carbon, nitrogen and oxygen. Hence, they easily degrade under the prevailing atmospheric conditions. Therefore, to know the extent of degradation, the prepared nanocomposites were tested for biodegradation using the soil burial test. The extent of degradation was calculated by measuring the mass loss compared to the initial weight of the sample. The soil burial test was conducted according to the procedure reported earlier, with slight modifications.[42] The film samples of about 20 mm × 20 mm were initially dried at 70° and weighed. The dried samples were placed under the soil at a depth of 10 cm. The soil was moistened by spraying water. After 15 days, the film samples were removed from the soil. The adhered soil was removed by washing with water and dried at 70°. Again, the weight of the samples was noted. The extent of degradation was calculated using the following formula:

$$\text{Biodegradation}(\%) = \frac{(W_1 - W_2)}{W_1} \times 100 \qquad (3)$$

where W_1 is the initial mass of the dry film, W_2 is the mass of the film after soil burial, respectively.

3.11. Overall migration rate (OMR)

The overall migration studies of the PGGA films were conducted in accordance with IS 9845:1998. Deionized water, 3% (v/v) acetic acid (CH_3COOH), and 50% (v/v) ethanol (C_2H_5OH) were used as food simulants representing aqueous, acidic, and alcoholic food systems, respectively. Pre-weighed active film samples (20 × 20 mm^2) were immersed in 30 mL of each simulant and incubated in a hot air oven at 40 °C for 10 days. After the exposure period, the simulants were analyzed to determine the overall migration, and the results were expressed in mg dm^{-2}.

3.12. Packaging studies

Application studies on fresh coriander leaves were conducted to evaluate the practical performance of the developed films under ambient conditions. Detailed experimental procedures and analyses are provided in the SI.

3.13. Statistical analysis

The obtained results were expressed as mean ± SD. The results were interpreted using one-way analysis of variance (ANOVA). The Statistical Package for Social Sciences (SPSS 17.0 for Windows, SPSS Inc, Chicago, II, USA) was used for the statistical analysis. The 95% confidence interval ($p < 0.05$) was considered significant (Scheme 1).

4. Results and discussion

4.1. Characterisation of silver nanoparticles (AgNPs)

The *in situ* formation of AgNPs from PVA/GG/GGh blend solution was studied by SEM with energy dispersive X-ray spectroscopy (EDX), UV-visible spectroscopy and XRD methods, respectively. The results are depicted in Fig. 1. The visual change in the colour of the solution from colourless to reddish brown (Fig. 1 (d) and (e)) indicated the formation of colloidal AgNPs.[43] The position and shape of the peaks in the XRD diffractograms give a clear indication regarding the crystal structure of the obtained AgNPs. The appearance of characteristic diffraction patterns at $2\theta = 38.2°$, 44.6°, 46.2° and 64.4°, respectively, corresponds to the face centred cubic crystal structure of AgNPs. The particle size calculated using the Debye–Scherrer equation ranged between 17 and 40 nm. These values agree with the standard values reported in the literature (JCPDS card No. 01-087-0719).[4]

The occurrence of sharp peaks indicated the *in situ* formation of AgNPs using the polymer blend solution. The UV-visible spectra (UV-vis spectrophotometer (Model UV-1601)) exhibited a characteristic peak around 430 nm due to surface plasmon resonance, confirming the formation of AgNPs in the polymer blend solution.[44] The SEM image depicted aggregation of the AgNPs. The EDX graph, along with atom%, confirmed the formation of AgNPs.[32] Dynamic light scattering (DLS) was used to measure the hydrodynamic size of the prepared AgNPs with a Horiba Scientific SZ-100 instrument. The results depicted that the hydrodynamic size of the synthesised silver nanoparticles was 88.3 ± 3.6 nm. This fact may be attributed to the higher viscosity of the polymer blend solution, which restricted the migration of AgNPs after their formation and decreased the agglomeration. This facilitated the stabilization of AgNPs in the polymer blend solution.

4.2. Moisture adsorption (MA)

Usually, the tendency to adsorb moisture is higher in biopolymer-based blend films. Therefore, the addition of

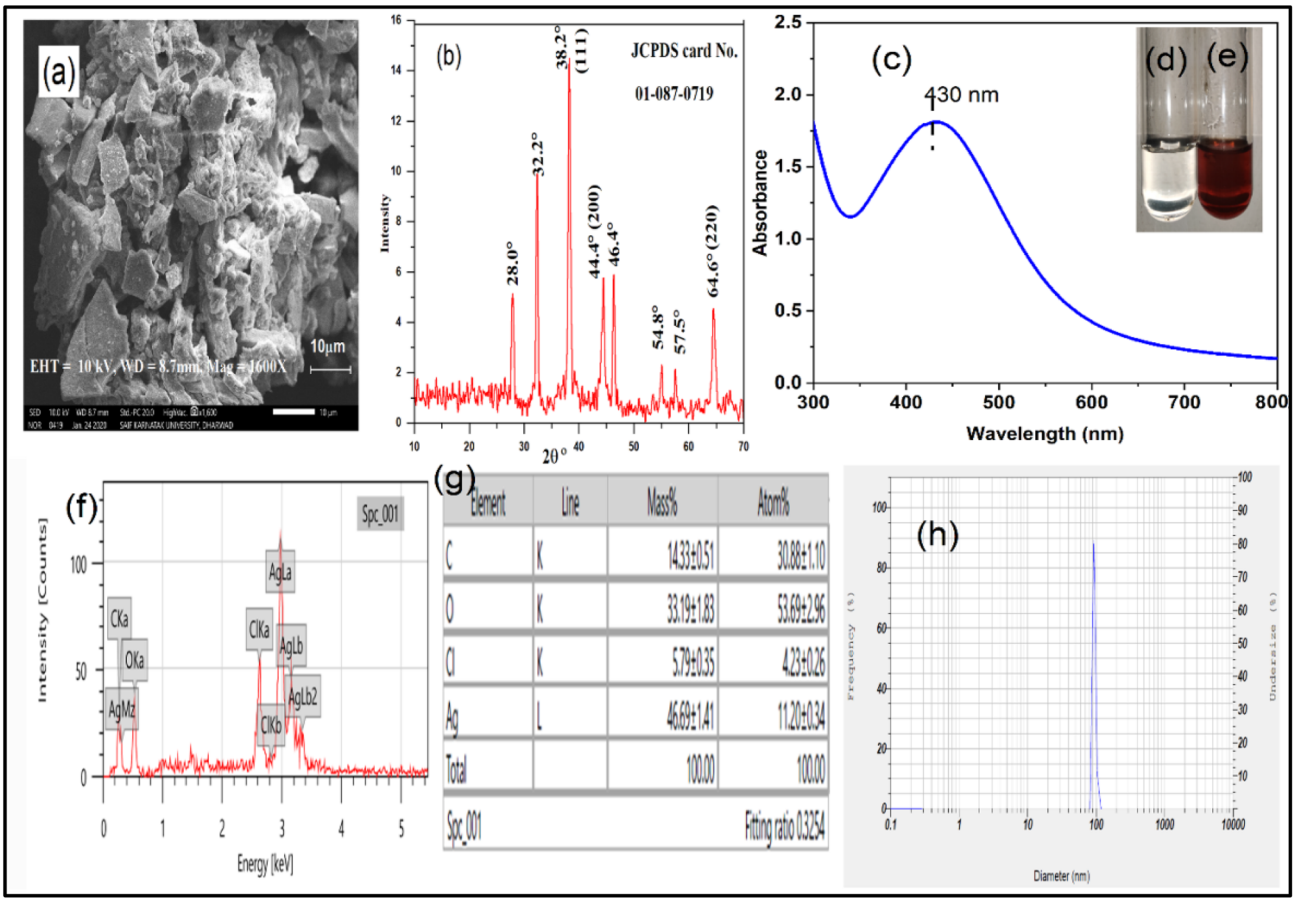

Fig. 1 (a) SEM image, (b) XRD diffractograms, (c) UV-visible spectra, (d) silver nitrate solution, (e) formation of AgNPs, (f) and (g) EDX spectra and atom% of AgNPs, and (h) DLS analysis of AgNPs.

nanoparticles is one such technique to minimize moisture adsorption, which is desirable for food packaging applications. Table 2 presents moisture adsorption for the PGGA-0 and PGGA nanocomposites. In the case of PGGA-0, the moisture adsorption was found to be 8.7 ± 0.4%. The presence of –OH groups on PVA, GG, GGh and glycerol can interact with water molecules *via* hydrogen bond formation that assists in the adsorption of water molecules on the surface.[45] There was an observed decrease in the moisture adsorption for the PGGA nanocomposites with an increase in the AgNP content. Among the studied compositions, PGGA-4 with higher AgNP content has shown less MA.[46] This decrease in water adsorption capacity suggested that the addition of AgNPs to the polymer matrix leads to the formation of a compact structure by the interaction of nanoparticles with the polymers.[46] This interaction is brought about by the formation of hydrogen bonding with polar groups of the polymer and AgNPs, which decreases the flexibility of the polymer chain and inhibits the interaction of –OH groups with water molecules.[38]

This reduction in moisture adsorption is directly correlated with improvements in water vapor transmission rate (WVTR). Lower water uptake decreases the affinity of the film toward environmental humidity, thereby reducing water vapor permeation through the matrix. Additionally, the formation of a compact structure and possible tortuous pathways created by well-dispersed AgNPs hinder the diffusion of gas molecules, contributing to improved oxygen barrier properties. The combined reduction in WVTR and oxygen transmission rate (OTR) enhances the suitability of the developed nanocomposite films for fruit packaging applications, where controlled moisture and oxygen transmission are critical for regulating respiration rate, minimizing weight loss, and extending shelf life.

4.3. Water contact angle (WCA) measurement

The study of the surface wettability of the films is desirable to find their suitability in various fields. Hydrophilic surfaces have a contact angle of >90°. The results of water contact angle measurements for PGGA-0 and PGGA nanocomposites are mentioned in Fig. 2. The PGGA-0 film exhibited a contact angle of 63.1 ± 2.1°. Since it contains polymers such as PVA, GG and GGh, which have a hydrophilic character due to the presence of plenty of –OH groups that can interact with water molecules, a hydrophilic surface is formed. PGGA nanocomposites showed enhanced hydrophobic character compared to the PGGA-0 film. This fact may be attributed to the presence of hydrophobic AgNPs, which increased the surface hydrophobicity. There was a slight increase in the contact angle for PGGA-1 (63.6 ± 3.3°). The lower AgNP content (0.05%) slightly increased the hydrophobic character of the film surface by forming hydrogen bonds with the polar functional groups of the polymers in the nanocomposites.[44] The highest contact angle of 96.3 ± 2.5° was observed for the PGGA-2 nanocomposite. Thereafter, the WCA values were found to be decreased for PGGA-3 and PGGA-4. Analysis of the results indicated that the major disadvantage of water-soluble polymers is their hydrophilicity, which can be conveniently overcome by forming nanocomposites with *in situ*-generated AgNPs.[48] As the concentration was increased, clusters of AgNPs were unequally distributed, causing a low contact angle.[44]

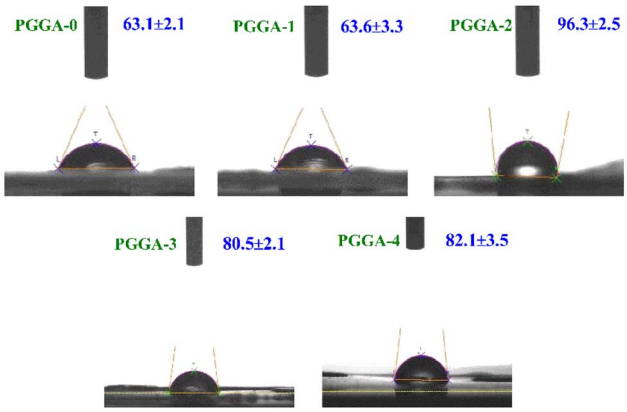

Fig. 2 WCA results of PGGA-0 and PGGA nanocomposites.

Table 2 Tensile strength (TS), elongation at break (EB), and moisture adsorption values of PGGA-0 and PGGA nanocomposites[a]

Sample code	Tensile strength (MPa)	Elongation at break (%)	Moisture adsorption (%)
PGGA-0	15.6 ± 0.5	189 ± 9	8.7 ± 0.4
PGGA-1	7.0 ± 2.1	133 ± 6	4.1 ± 0.2
PGGA-2	5.9 ± 1.5	122 ± 4	4.1 ± 0.2
PGGA-3	5.8 ± 0.9	73 ± 3	4.5 ± 0.3
PGGA-4	5.8 ± 0.6	136 ± 5	2.2 ± 0.1

[a] Values are given as mean ± SD ($n = 3$).

4.4. Mechanical properties

The study of the mechanical properties gives insight into the ability to withstand stress during handling, which is very crucial for packaging applications. The TS and EB were studied to understand the impact of AgNPs on the PGGA nanocomposites, and the results are given in Table 2. The measured TS and EB for control film PGGA-0 were 15.6 ± 0.5 MPa and 189 ± 9%, respectively. The incorporation of AgNPs into the polymer matrix resulted in a slight decrease in the TS for PGGA nanocomposites.[49]

Elongation at break refers to the extent of entanglement of polymers with AgNPs, and a slightly increased EB indicates enhanced flexibility. The results of EB also decreased from PGGA-1 to PGGA-3, while showing a higher value for PGGA-4. The presence of AgNPs caused a decrease in EB due to restricted polymer chain movement.[50] The incorporation of AgNPs produced less flexible films, confirming the reinforcing effect of AgNPs in the polymer matrix.[26] The homogeneous distribution of AgNPs caused rigidity and stiffness of the polymer chain. The presence of an excess of AgNPs may break the hydrogen bond formation, reducing the TS of the nanocomposites, while an increase in EB was observed.[45]

4.5. Fourier transform infrared (FTIR) spectroscopy

FTIR is used to investigate the changes associated with the structure during the formation of nanocomposites.[51] The FTIR spectra of PGGA-0 and PGGA nanocomposites are depicted in Fig. 3. The spectra of PGGA-0 showed the stretching vibration for the –OH group at 3263 cm^{-1}. The peaks at 2938 cm^{-1} and 1647 cm^{-1} correspond to –CH stretching vibration and –C=O stretching vibration of the acetyl group, respectively. The FTIR spectra of PGGA nanocomposites also recorded similar peaks as observed in PGGA-0.

In the case of PGGA nanocomposites, the absorption bands in the range of 3287–3279 cm^{-1} are attributed to –OH stretching vibration.[52] The peaks at 2940 cm^{-1}–2938 cm^{-1} are ascribed to the –CH stretching vibration of the $-CH_2$ group.[4] The occurrence of a peak around 1714 cm^{-1}–1712 cm^{-1} was due to the presence of the –C=O group of free carboxylic acid and glucuronic acid esters of gum ghatti.[2] However, minor shifts in the peak values have been observed for the –OH group and –C=O stretching due to the inclusion of AgNPs. As can be observed, the peaks at 1712 cm^{-1} and 3287 cm^{-1} are slightly shifted to higher wave numbers in the nanocomposites due to the formation and entrapment of AgNPs in the PGGA nanocomposites.[26] The increased broadness of the peak around 3287 cm^{-1}–3279 cm^{-1} suggested the formation of the hydrogen bond between the AgNPs and components of the polymer matrix.[18] The band at 827 cm^{-1} was attributed to the -O–Ag bond formed by the interaction of Ag with the –OH group of the polymers and glycerol in the polymer nanocomposites.[45] Apart from this, the position of the peaks for PGGA-0 and PGGA nanocomposites occurred at the same position, indicating the absence of chemical interaction between AgNPs and the polymer matrix.[44] The FTIR spectra of AgNPs (Fig. 2 and c) suggested

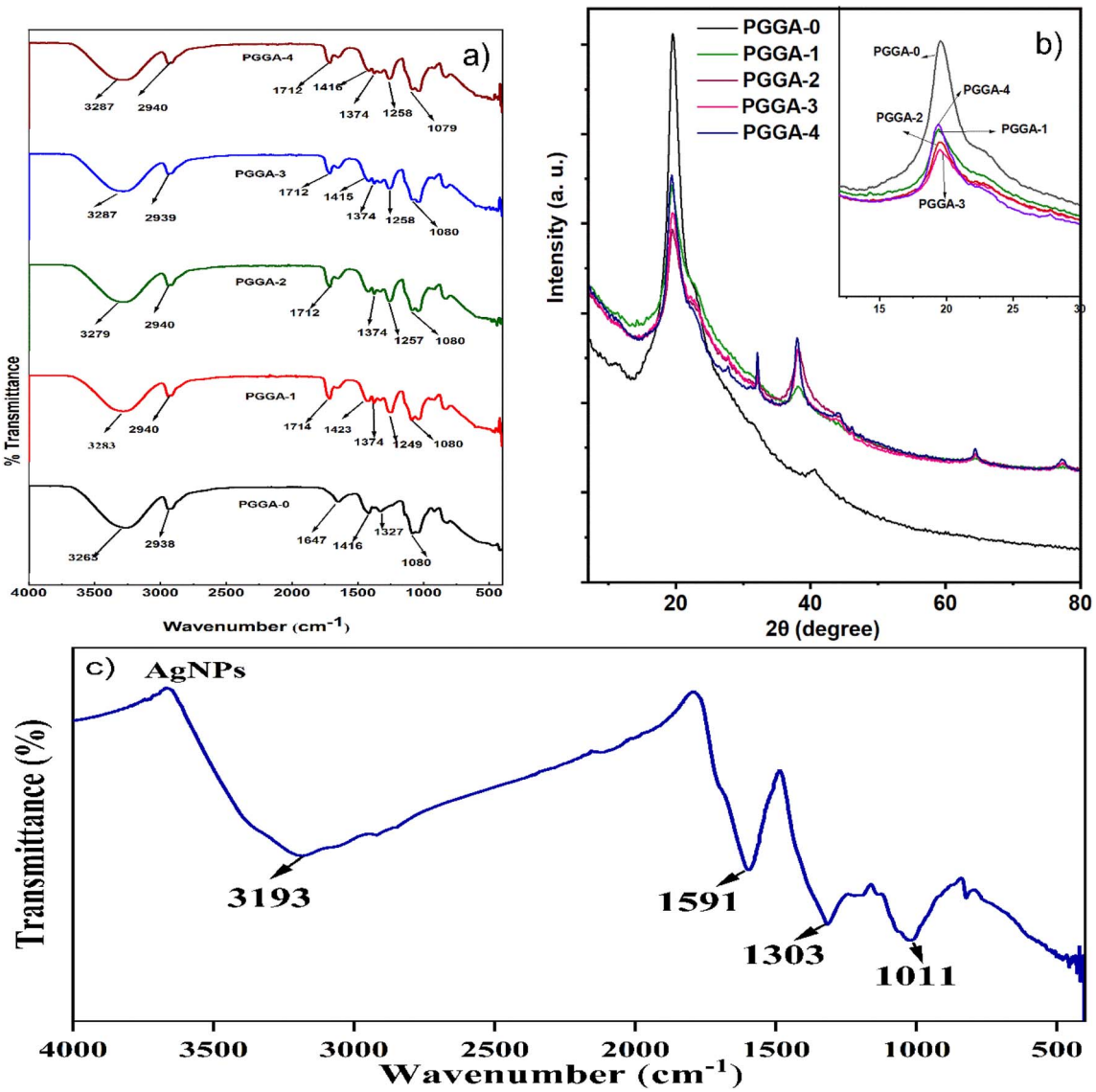

Fig. 3 (a) FTIR spectra of PGGA-0 and PGGA nanocomposites, (b) XRD patterns of PGGA-0 and PGGA nanocomposites, and (c) FTIR spectra of AgNPs.

the presence of peaks at 3193 cm^{-1}, 1591 cm^{-1} and 1011 cm^{-1}, which were ascribed to stretching vibration of –OH, C=O, and C–O functional groups, indicating the role of –OH and C=O functional groups of GG, PVA and GGh in reducing Ag^{+} to AgNPs.[47] This fact clearly indicated that the presence of sugar and –OH groups is responsible for reducing and stabilising the formation of AgNPs.[53]

4.6. Scanning electron microscopy (SEM)

The changes in the surface morphology of PGGA nanocomposites with different concentrations of AgNPs have been studied with reference to the PGGA-0 film (Fig. 4). The surface microstructure of PGGA-0 showed a smooth and compact structure without pores. The SEM images of PGGA nanocomposites showed the presence of some aggregated particles on the surface, which was due to the presence of guar gum.[23] When AgNPs were incorporated in the polymer matrix, roughness was observed on the surface, along with the dispersion of AgNPs indicated by white particles. This fact indicated that the polymer blend mediated the *in situ* formation of AgNPs.[26] As the concentration of AgNPs increased, there was an observed increase in the dispersion of white particles,[54] suggesting encapsulation of AgNPs in the polymer matrix (Fig. 5). Arfat *et al.* observed a similar type of rough surface morphology in GG/Ag-Cu nanocomposite films.[26]

4.7. X-ray diffraction (XRD) analysis

The XRD patterns for the PGGA-0 film and PGGA nanocomposites are displayed in Fig. 3. For the PGGA-0 film, a prominent broad peak was observed at $2\theta = 19.53°$ due to the semicrystalline nature of PVA, and diffraction for other polymers superimposed at the same Bragg's angle.[55] The PGGA nanocomposites showed, along with a broad peak, intense diffraction peaks at 2θ = 38.4°, 44.3°, and 64.5° respectively, indexed as the (111), (200) and (220) planes of crystalline AgNPs in PGGA nanocomposites, indicating the presence of AgNPs in the polymer matrix.[2,56] The presence of AgNPs in the polymer matrix decreased the peak height, indicating an increased amorphous region in the polymer matrix.[53] Energy Dispersive X-ray (EDX) analysis was used for the study of the elemental composition of the nanocomposites (Fig. 4). The fingerprint of each energy line gives information regarding the composition of each element.[17] It is clear from the spectra that PGGA-0 depicted a signal for C and O (51% and 49% w/w, respectively) due to the presence of polymers PVA/GG/GGh. The analysis of EDX spectra of PGGA nanocomposites revealed the presence of a signal at 3 KeV for AgNPs, along with the presence of carbon and hydrogen, which indicated *in situ* formation of AgNPs using PVA/GG/GGh blend solution.[57,58] The results indicated an increase in the concentration of AgNPs with an increase in the concentration of silver nitrate.[59]

4.8. Thermogravimetric analysis (TGA)

TGA is used to study thermal degradation or thermal stability as a function of temperature.[60] Therefore, thermogravimetric (TG) curves were recorded to study the influence of AgNPs on the thermal properties and thermal stability of the PGGA nanocomposites. The results of the thermogravimetric analysis are presented in Fig. 6(a). The thermogram of the PGGA-0 and PGGA nanocomposites showed three stages of weight loss attributed to moisture loss, structural deterioration, degradation of PVA and oxidative decomposition of the polymer chains, respectively.[18] In the case of PGGA-0, the initial stage of degradation occurred around 100 °C due to moisture loss.

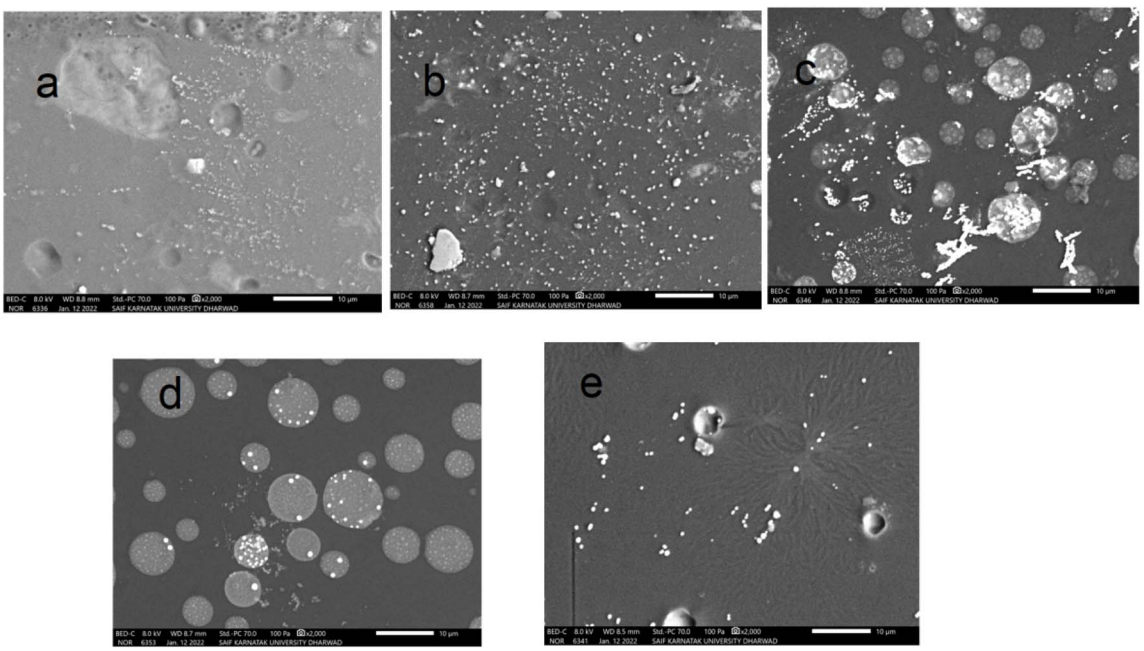

Fig. 4 SEM images of (a) PGGA-0, (b) PGGA-1, (c) PGGA-2, (d) PGGA-3 and (e) PGGA-4 nanocomposites.

a)

	Element	Line	Mass%	Atom%
a)	C	K	51.06±0.17	58.26±0.19
	O	K	48.41±0.43	41.47±0.37
	Na	K	0.35±0.04	0.21±0.02
	K	K	0.18±0.02	0.06±0.01
	Total		100.00	100.00
	Spc_001			Fitting ratio 0.0506

	Element	Line	Mass%	Atom%
b)	C	K	54.56±0.20	62.44±0.23
	O	K	43.42±0.50	37.30±0.43
	Ag	L	2.02±0.09	0.26±0.01
	Total		100.00	100.00
	Spc_001			Fitting ratio 0.0606

	Element	Line	Mass%	Atom%
c)	C	K	51.52±0.16	60.39±0.19
	O	K	44.24±0.43	38.93±0.38
	Al	K	0.22±0.02	0.11±0.01
	Ca	K	0.16±0.03	0.06±0.01
	Ag	L	3.86±0.10	0.50±0.01
	Total		100.00	100.00
	Spc_001			Fitting ratio 0.0513

	Element	Line	Mass%	Atom%
d)	C	K	51.85±0.16	61.32±0.19
	O	K	42.54±0.41	37.77±0.37
	Na	K	0.29±0.03	0.18±0.02
	Ca	K	0.18±0.03	0.06±0.01
	Ag	L	5.14±0.11	0.68±0.01
	Total		100.00	100.00
	Spc_001			Fitting ratio 0.0487

	Element	Line	Mass%	Atom%
e)	C	K	49.71±0.16	60.28±0.20
	O	K	42.47±0.44	38.66±0.40
	Ag	L	7.82±0.14	1.06±0.02
	Total		100.00	100.00
	Spc_001			Fitting ratio 0.0583

b)

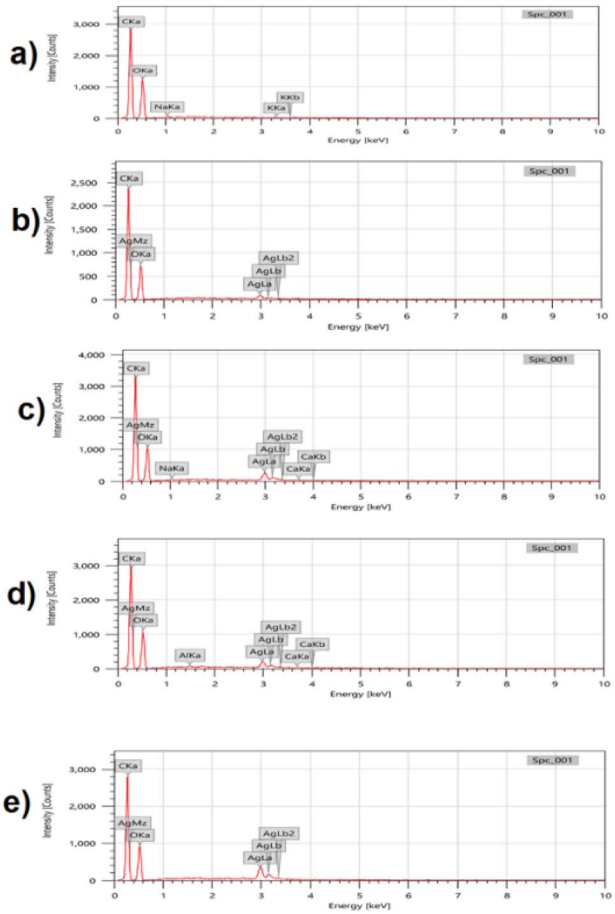

Fig. 5 (a) Atom% and (b) EDX analysis of (a) PGGA-0, (b) PGGA-1, (c) PGGA-2, (d) PGGA-3, and (e) PGGA-4 nanocomposites.

Subsequently, degradation was observed at 192 °C, which can be attributed to the breaking of polymer chains and the decomposition of glycerol used as a plasticizer.[18] The second stage of weight loss was attributed to the degradation of PVA that occurred around 318 C, and the third degradation phase around 427 C was associated with the oxidative decomposition of the polymer chains. In PGGA nanocomposites, major degradation occurred around 305–319 C with a cumulative

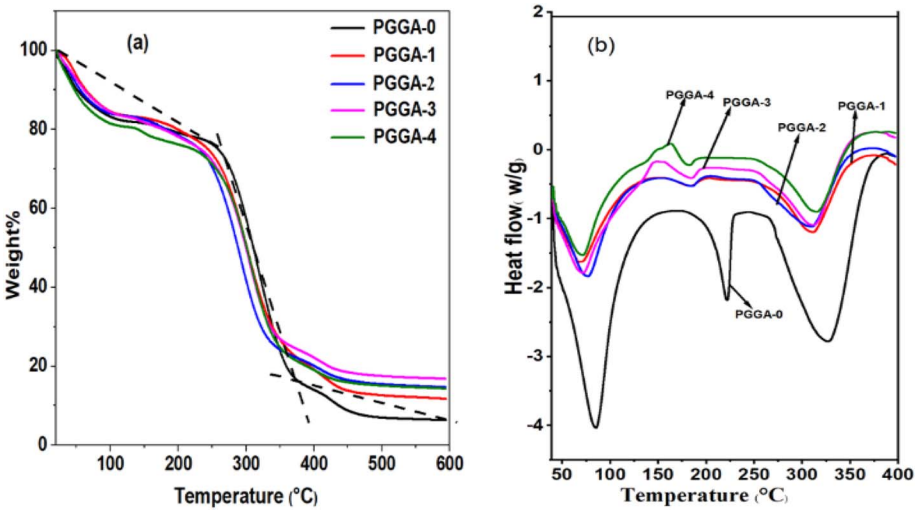

Fig. 6 (a) TGA and (b) DSC curves of PGGA-0 and PGGA nanocomposites.

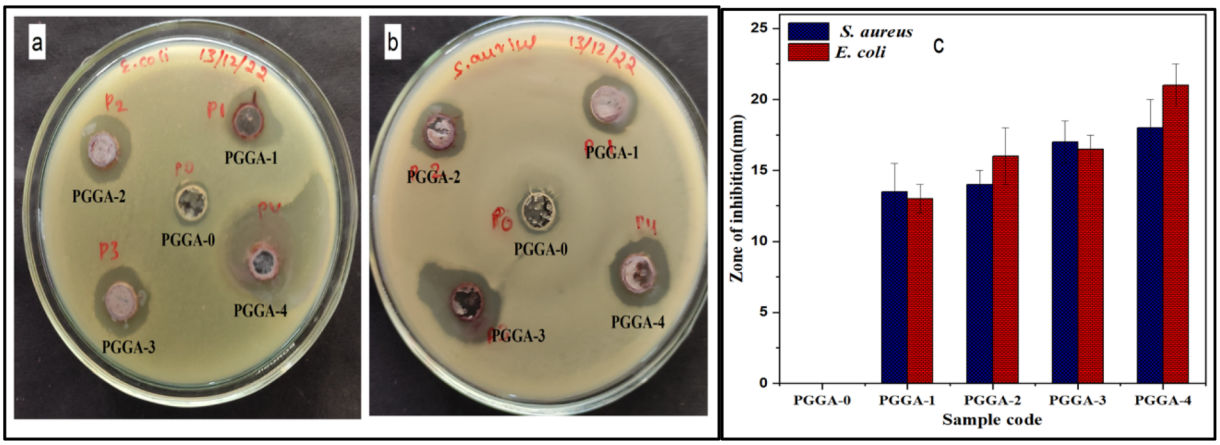

Fig. 7 (a) and (b) Images of the zone of inhibition and (c) diameter of zone of inhibition values of PGGA-0 and PGGA nanocomposites.

Table 3 Results of biodegradation and diameter of zone of inhibition values of PGGA-0 and PGGA nanocomposites[a]

Sample code	Biodegradation (%)	Zone of inhibition diameter	
		S. aureus (mm)	*E. coli* (mm)
PGGA-0	12.2 ± 1.2	0 ± 0	0 ± 0
PGGA-1	21.2 ± 0.5	13.5 ± 2	13 ± 1
PGGA-2	14.1 ± 0.9	14 ± 1	16 ± 2
PGGA-3	12.6 ± 1.5	17 ± 1.5	16.5 ± 1
PGGA-4	13.5 ± 1.0	18 ± 2	21 ± 1.5

[a] Values are given as mean ± SD ($n = 3$).

mass loss of 57–62% due to thermal decomposition of the PGGA nanocomposites, suggesting better thermal stability above 200 C.[61] It was observed that around 400 C, the residue left for PGGA nanocomposites was higher than that of the PGGA-0 film. This observation suggested that the weight loss was influenced by the concentration of AgNPs in the PGGA nanocomposites. The increase in the weight of the residue for the PGGA nanocomposites compared to the PGGA-0 film was due to thermally stable AgNPs. It is to be noted that the amount of residue left was greater than the AgNP content in the nanocomposites, suggesting that the inclusion of AgNPs improved the thermal stability of PGGA nanocomposites.[18,45]

4.9. Differential scanning calorimetry (DSC)

DSC curves of PGGA-0 and PGGA nanocomposites are depicted in Fig. 6(b). In the case of PGGA-0, the glass transition temperature was observed at 64 C. The first broad endothermic curve observed at 85.7 C associated with the removal of moisture content with an enthalpy of 613.2 J g^{-1}. The 2nd endothermic peak for the melting temperature occurred at 222 C with an enthalpy of 123.3 J g^{-1}. The thermograms for PGGA nanocomposites have shown a single endothermic peak between 71.2 C and 77.5 C, suggesting compatibility among AgNPs and the polymer matrix. The results obtained for nanocomposites showed decreased T_g with the incorporation of AgNPs. The melting temperature and melting enthalpy of nanocomposites decreased slightly with the incorporation of nanoparticles.[57] This observation may be associated with the fact that with an increase in the concentration of AgNPs in the polymer matrix, there is a reduction in the free volume and increased compactness of the resulting structure.[10] The results obtained are in agreement with the earlier literature and indicate better thermal stability for PGGA nanocomposites.[62]

4.10. Antibacterial properties

Active packaging with antibacterial properties grabbed considerable attention for the packaging of food products. These packaging materials could inhibit the growth of pathogens, thus preventing the spoilage of food products.[63,64] Since AgNPs are known for their antibacterial activity, they can find applications in food packaging and the medical field as antibacterial agents. The agar well diffusion method was used to evaluate the antibacterial activity of PGGA nanocomposites against two bacterial strains, *viz.*, *S. aureus* and *E. coli*. The values and images of the inhibition zone diameter for the samples are mentioned in Fig. 7 and Table 3. The PGGA-0 film has not shown an inhibition zone for *S. aureus* and *E. coli* bacteria, respectively, implying no antibacterial activity. Similar findings were also reported in the earlier literature that the presence of PVA, GG and GGh did not show antibacterial activity against tested microorganisms.[23,52] There was an observable improvement in the zone of inhibition for PGGA compared to PGGA-0 due to the presence of AgNPs.[44] It shows that the presence of AgNPs effectively inhibited the growth of bacteria. The results suggested that the zone of inhibition observed for *E. coli* was higher than that for *S. aureus* bacteria.[65] Several theories have been mentioned to give a satisfactory explanation for the difference in the antibacterial action against this tested microorganism. AgNPs produce active oxygen species that react with bacterial proteins and DNA, which are capable of destroying the thin outer membrane of *E. coli*.[66] *S. aureus* has a thick cell wall structure that was not easily attacked by AgNPs. The results obtained indicated that an increase in AgNP content increased

Table 4 Results of overall migration of PGGA-0 and PGGA nanocomposites[a]

Sample code	Overall migration as per IS: 9845–1998		
	Deionised water 10 days at 40 °C (mg dm^{-2})	3% CH_3COOH 10 days at 40 °C (mg dm^{-2})	50% C_2H_5OH 10 days at 40 °C (mg dm^{-2})
PGGA-0	14.4 ± 1.1	11.5 ± 0.9	12.4 ± 0.3
PGGA-1	7.5 ± 0.8	8.4 ± 0.6	7.4 ± 0.8
PGGA-2	7.2 ± 0.1	5.1 ± 0.1	7.2 ± 0.4
PGGA-3	6.9 ± 0.2	5.0 ± 0.2	6.4 ± 0.1
PGGA-4	6.5 ± 0.1	4.2 ± 0.3	6.1 ± 0.2

[a] Values are given as mean ± SD ($n = 3$).

the effectiveness in inhibiting the growth of bacteria. Therefore, the AgNPs present in the nanocomposites are capable of inhibiting the growth of the microorganisms and can be considered as an active film with antibacterial properties.

4.11. Soil burial test

The increasing awareness regarding environmental pollution created by waste disposal of packaging material has led to the development and application of biodegradable packaging materials.[67,68] The soil burial degradation test was carried out to study the degradation of the PGGA nanocomposites, and the results are mentioned in Table 3. The results showed biodegradation of the PGGA-0 and PGGA nanocomposites. The polymers PVA, GG and GGh are hydrophilic in nature; partial dissolution and degradation in the presence of moisture by microorganisms present in the soil are responsible for the weight loss of the PGGA nanocomposites.[69]

4.12. Overall migration study

The performance of the PGGA-0 film and PGGA nanocomposites for food packaging applications was evaluated through overall migration studies using three food simulants: deionised water, 3% CH_3COOH, and 50% C_2H_5OH, representing aqueous, acidic, and alcoholic food systems, respectively. Migration testing is crucial to assess the safety and suitability of packaging materials, as the transfer of film components into food systems may result in contamination. As per BIS standard IS: 9845–1998, the overall migration from packaging materials must not exceed 10 mg dm^{-2}.[69]

The overall migration values of the developed films are summarized in Table 4. All PGGA nanocomposite films demonstrated migration levels well below the regulatory limit of 10 mg dm^{-2} in each of the three simulants, indicating their compliance for food contact applications.[88,89] Relatively higher migration was observed in 3% CH_3COOH, compared to deionised water and 50% C_2H_5OH, which may be attributed to stronger interactions between the acidic medium and the PGGA matrix, leading to increased swelling or partial structural relaxation. Furthermore, the incorporation of silver nanoparticles (AgNPs) into the PGGA matrix reduced the overall migration in all simulants, likely due to enhanced matrix compactness, improved intermolecular interactions, and the barrier effect imparted by the nanoparticles, which restricts the diffusion of migratory substances. Table 5 encompasses some of the existing literature with the present work.

Green synthesis of AgNPs was carried out using a polymer blend solution of PVA/GG/GGh at room temperature. The AgNP-incorporated PGGA nanocomposites were prepared by a simple solvent casting technique. The characteristic peaks observed in the XRD diffractogram at $2\theta = 38.2°$, 44.6°, 46.2° and 64.4°, respectively, confirmed the formation of AgNPs. Uniform dispersion of AgNPs into the polymer matrix was evidenced by SEM analysis, suggesting good compatibility among the AgNPs and the polymer matrix. There was an improvement in the hydrophobicity (63.6 ± 3.3° to 96.3 ± 2.5°) and elongation at break (133 ± 6 to 136 ± 5%) for PGGA nanocomposites compared to the PGGA-0 film.[87] The study of FTIR supported the hydrogen bonding interaction between AgNPs and the polymer matrix. Dispersion of AgNPs into the polymer matrix confirmed

Table 5 Comparing the key properties of the present work with existing literature

Sl No	Matrix	Active agent	Mechanical properties	Antibacterial properties	Ref.
1	Guar gum/ PVA composite	Silver nanoparticles (AgNPs)	Not focused on film tensile data (nanoparticles synthesized and characterized; particle size 2–18 nm by TEM)	Active against *S. aureus*, *E. coli*, and *P. aeruginosa* (clear inhibition zones observed)	[70]
2	PVA/Guar gum film (PGS series)	*In situ* AgNPs (3.4–13.6 mg)	TS improved up to 23.93 MPa (optimal at PGS2); enhanced thermal stability (~61%); improved hydrophobicity (~77%)	Effective against *S. aureus* and *E. coli*; clear inhibition zones reported; no activity in control film	[71]
3	Chitosan/Guar gum/ Gum ghatti (CGGA series)	*In situ* AgNPs (0.05–0.2 wt%)	TS increased from 8.2 ± 0.5 MPa (control) to 30.7 ± 2.2 MPa; improved hydrophobicity (79° → 92°); reduced swelling & moisture adsorption	Strong antibacterial activity against *S. aureus* and *E. coli*; clear inhibition zones due to synergistic AgNP-polymer effect	[72]
4	Present work	*In situ* AgNPs	TS: 5.8 ± 0.6 MPa; EB: 136 ± 5%	*S. aureus* 18 ± 2 mm; *E. coli* 21 ± 1.5 mm	—

decreased crystallinity in PGGA nanocomposites, which were manifested in the XRD study. Inclusion of AgNPs into the polymer matrix decreased moisture adsorption form 4.1 ± 0.2 to 2.2 ± 0.1% and improved thermal stability of the PGGA nanocomposites. The miscibility of the constituents was evidenced by the occurrence of a single glass transition temperature. The presence of AgNPs in the PGGA nanocomposites improved the resistance to the growth of bacteria. Furthermore, among the nanocomposites, PGGA-4 has shown better surface homogeneity, hydrophobicity and antibacterial properties. All these results suggested that PGGA nanocomposites with green-synthesised AgNPs are environmentally friendly, cost-effective and convenient to use in food packaging.

Author contributions

Veena G. Bhat: conceptualization, data interpretation, writing – original manuscript. Saraswati P. Masti: supervision, corresponding author, review, formal correction. Shivayogi S. Narasagoudr: data curation, formal analysis. Lingaraj Kariyappa Kurabetta: data interpretation, formal analysis, analysis of data. Manjushree Nagaraj Gunaki: formal analysis, design of study, data curation, investigation. Ajitkumar Appayya Hunashyal: data curation, formal analysis. Ravindra B. Chougale: revising manuscript. Ravindra B. Malabadi: analysis of data.

Conflicts of interest

The authors declare that they have no possible competing financial interests or personal relationships that could have appeared to influence the work reported in this paper.

Data availability

The data supporting the findings of this study are available from the corresponding author upon reasonable request.

Supplementary information (SI) is available. See DOI: https://doi.org/10.1039/d5fb00825e.

Acknowledgements

Dr Saraswati P. Masti, Principal Investigator of the DST-SERB project, would like to thank the DST-SERB for providing financial assistance under project sanction letter No. SB/EMEQ-213/2014, dated: 29-01-2016. The authors also express their gratitude to the Principal and the HOD, Chemistry, Karnatak Science College, Dharwad, for providing infrastructure facilities. Furthermore, the authors extend profound gratitude to the University Scientific and Instrumentation Centre (USIC), Karnatak University, DST Sophisticated Analytical Instrument Facilities (SAIF), Dharwad, for instrument facilities. The authors also acknowledge DST, New Delhi, for extending the instrument facilities under the DST-PURSE Phase-II program [Grant No. SR/PURSEPHASE-2/13(G)].

References

1 N. Khan, D. Kumar and P. Kumar, Silver nanoparticles embedded guar gum/gelatin nanocomposite: Green synthesis, characterization and antibacterial activity, *Colloid Interface Sci. Commun.*, 2020, **35**, 100242.
2 G. Babaladimath and V. Badalamoole, Silver nanocomposite hydrogel of Gum Ghatti with potential antibacterial property, *J. Macromol. Sci., Pure Appl. Chem.*, 2019, **56**(10), 952–959.
3 M. Hoseinnejad, S. M. Jafari and I. Katouzian, Inorganic and metal nanoparticles and their antimicrobial activity in food packaging applications, *Crit. Rev. Microbiol.*, 2018, **44**(2), 161–181.
4 J. Balachandramohan and T. Sivasankar, Sonication-assisted synthesis of a new heterostructured schiff base ligand Silver-Guar gum encapsulated nanocomposite as a visible light photocatalyst, *J. Microencapsulation*, 2020, **37**(1), 29–40.
5 J. Singh and A. Dhaliwal, Synthesis, characterization and swelling behavior of silver nanoparticles containing superabsorbent based on grafted copolymer of polyacrylic acid/Guar gum, *Vacuum*, 2018, **157**, 51–60.
6 M. S. K. Sofla, S. Mortazavi and J. Seyfi, Preparation and characterization of polyvinyl alcohol/chitosan blends plasticized and compatibilized by glycerol/polyethylene glycol, *Carbohydr. Polym.*, 2020, **232**, 115784.
7 T. Das, S. Yeasmin, S. Khatua, K. Acharya and A. Bandyopadhyay, Influence of a blend of guar gum and poly (vinyl alcohol) on long term stability, and antibacterial and antioxidant efficacies of silver nanoparticles, *RSC Adv.*, 2015, **5**(67), 54059–54069.
8 S. R. Kanatt and S. H. Makwana, Development of active, water-resistant carboxymethyl cellulose-poly vinyl alcohol-Aloe vera packaging film, *Carbohydr. Polym.*, 2020, **227**, 115303.
9 S. S. Narasagoudr, V. G. Hegde, V. N. Vanjeri, R. B. Chougale and S. P. Masti, Influence of Boswellic acid on Physical, Structural and Morphological Properties of Poly (vinyl alcohol) Films, *Chem. Data Collect.*, 2020, 100370.
10 T. Gasti, V. D. Hiremani, S. S. Kesti, V. N. Vanjeri, N. Goudar, S. P. Masti, S. C. Thimmappa and R. B. Chougale, Physicochemical and antibacterial evaluation of poly (vinyl alcohol)/guar gum/silver nanocomposite films for food packaging applications, *J. Polym. Environ.*, 2021, **29**(10), 3347–3363.
11 S. Hajji, A. Chaker, M. Jridi, H. Maalej, K. Jellouli, S. Boufi and M. Nasri, Structural analysis, and antioxidant and antibacterial properties of chitosan-poly (vinyl alcohol) biodegradable films, *Environ. Sci. Pollut. Res.*, 2016, **23**(15), 15310–15320.
12 M. S. Amiri, V. Mohammadzadeh, M. E. T. Yazdi, M. Barani, A. Rahdar and G. Z. Kyzas, Plant-Based Gums and Mucilages Applications in Pharmacology and Nanomedicine: A Review, *Molecules*, 2021, **26**(6), 1770.

13 Q. Yuan and T. D. Golden, A novel method for synthesis of clay/polymer stabilized silver nanoparticles, *Surf. Interfaces*, 2020, **20**, 100620.
14 R. Kalaivani, M. Maruthupandy, T. Muneeswaran, A. H. Beevi, M. Anand, C. Ramakritinan and A. Kumaraguru, Synthesis of chitosan mediated silver nanoparticles (Ag NPs) for potential antimicrobial applications, *Front. Lab. Med.*, 2018, **2**(1), 30–35.
15 Y. Zheng, Y. Zhu, G. Tian and A. Wang, In situ generation of silver nanoparticles within crosslinked 3D guar gum networks for catalytic reduction, *Int. J. Biol. Macromol.*, 2015, **73**, 39–44.
16 P. Velusamy, J. Das, R. Pachaiappan, B. Vaseeharan and K. Pandian, Greener approach for synthesis of antibacterial silver nanoparticles using aqueous solution of neem gum (Azadirachta indica L.), *Ind. Crop. Prod.*, 2015, **66**, 103–109.
17 E. Ugwoke, S. O. Aisida, A. A. Mirbahar, M. Arshad, I. Ahmad, T.-k. Zhao and F. I. Ezema, Concentration induced properties of silver nanoparticles and their antibacterial study, *Surf. Interfaces*, 2020, **18**, 100419.
18 A. Venkateshaiah, J. Y. Cheong, C. Habel, S. Wacławek, T. Lederer, M. Cernik, I.-D. Kim, V. V. Padil and S. Agarwal, Tree gum–graphene oxide nanocomposite films as gas barriers, *ACS Appl. Nano Mater.*, 2019, **3**(1), 633–640.
19 C. M. Araújo, M. das Virgens Santana, A. do Nascimento Cavalcante, L. C. C. Nunes, L. C. Bertolino, C. A. R. de Sousa Brito, H. M. Barreto and C. Eiras, Cashew-gum-based silver nanoparticles and palygorskite as green nanocomposites for antibacterial applications, *Mater. Sci. Eng. C*, 2020, **115**, 110927.
20 M. K. Indana, B. R. Gangapuram, R. Dadigala, R. Bandi and V. Guttena, A novel green synthesis and characterization of silver nanoparticles using gum tragacanth and evaluation of their potential catalytic reduction activities with methylene blue and Congo red dyes, *J. Anal. Sci. Technol.*, 2016, **7**(1), 1–9.
21 R. Singh, H. Priya, S. R. Kumar, D. Trivedi, N. Prasad, F. Ahmad, J. G. Chengaiyan, S. Haque and S. S. Rana, Gum Ghatti: A Comprehensive Review on Production, Processing, Remarkable Properties, and Diverse Applications, *ACS Omega*, 2024, **9**, 9974–9990.
22 T. Cheng, J. Xu, Y. Li, Y. Zhao, Y. Bai, X. Fu, X. Gao and X. Mao, Effect of gum ghatti on physicochemical and microstructural properties of biodegradable sodium alginate edible films, *J. Food Meas. Char.*, 2021, **15**, 107–118.
23 S. S. Narasagoudr, S. P. Masti, V. G. Hegde and R. B. Chougale, Cetrimide Crosslinked Chitosan/Guar Gum/Gum Ghatti Active Biobased Films for Food Packaging Applications, *J. Polym. Environ.*, 2022, 1–16.
24 R. R. Palem, G. Shimoga, T. J. Kang and S.-H. Lee, Fabrication of multifunctional Guar gum-silver nanocomposite hydrogels for biomedical and environmental applications, *Int. J. Biol. Macromol.*, 2020, **159**, 474–486.
25 S. Rahman, A. Konwar, G. Majumdar and D. Chowdhury, Guar gum-chitosan composite film as excellent material for packaging application, *Carbohydr. Polym. Technol. Appl.*, 2021, **2**, 100158.
26 Y. A. Arfat, M. Ejaz, H. Jacob and J. Ahmed, Deciphering the potential of guar gum/Ag-Cu nanocomposite films as an active food packaging material, *Carbohydr. Polym.*, 2017, **157**, 65–71.
27 D. N. Iqbal, M. Tariq, S. M. Khan, N. Gull, S. Sagar Iqbal, A. Aziz, A. Nazir and M. Iqbal, Synthesis and characterization of chitosan and guar gum based ternary blends with polyvinyl alcohol, *Int. J. Biol. Macromol.*, 2020, **143**, 546–554.
28 G. Sharma, S. Sharma, A. Kumar, H. Ala'a, M. Naushad, A. A. Ghfar, G. T. Mola and F. J. Stadler, Guar gum and its composites as potential materials for diverse applications: A review, *Carbohydr. Polym.*, 2018, **199**, 534–545.
29 M. P. Eelager, S. P. Masti, R. B. Chougale, V. D. Hiremani, S. S. Narasgoudar, N. P. Dalbanjan and P. K. SK, Evaluation of mechanical, antimicrobial, and antioxidant properties of vanillic acid induced chitosan/poly (vinyl alcohol) active films to prolong the shelf life of green chilli, *Int. J. Biol. Macromol.*, 2023, **232**, 123499.
30 B. Saberi, S. Chockchaisawasdee, J. B. Golding, C. J. Scarlett and C. E. Stathopoulos, Characterization of pea starch-guar gum biocomposite edible films enriched by natural antimicrobial agents for active food packaging, *Food Bioprod. Process.*, 2017, **105**, 51–63.
31 A. R. Taherian, P. Lacasse, B. Bisakowski, S. Lanctôt and P. Fustier, A comparative study on the rheological and thermogelling properties of chitosan/polyvinyl alcohol blends in dairy products, *LWT–Food Sci. Technol.*, 2019, **113**, 108305.
32 O. Velgosova, L. Mačák, E. Múdra, M. Vojtko and M. Lisnichuk, Preparation, Structure, and Properties of PVA–AgNPs Nanocomposites, *Polymers*, 2023, **15**(2), 379.
33 W. Guo, M. Yang, S. Liu, X. Zhang, B. Zhang and Y. Chen, Chitosan/polyvinyl alcohol/tannic acid multiple network composite hydrogel: Preparation and characterization, *Iran. Polym. J.*, 2021, **30**(11), 1159–1168.
34 Y. Sun, X. Jiang and L. Hou, A quaternized poly (vinyl alcohol)/chitosan composite alkaline polymer electrolyte: preparation and characterization of the membrane, *Iran. Polym. J.*, 2017, **26**, 531–539.
35 R. E. Esfahani, P. Zahedi and R. Zarghami, 5-Fluorouracil-loaded poly (vinyl alcohol)/chitosan blend nanofibers: morphology, drug release and cell culture studies, *Iran. Polym. J.*, 2021, **30**, 167–177.
36 A. CagriAta, Ü. Yildiko, İ. Cakmak and A. A. Tanriverdi, Synthesis and characterization of polyvinyl alcohol-g-polystyrene copolymers via MADIX polymerization technique, *Iran. Polym. J.*, 2021, **30**(9), 885–895.
37 A. Hassan, M. B. K. Niazi, A. Hussain, S. Farrukh and T. Ahmad, Development of anti-bacterial PVA/starch based hydrogel membrane for wound dressing, *J. Polym. Environ.*, 2018, **26**(1), 235–243.
38 V. G. Bhat, S. S. Narasagoudr, S. P. Masti, R. B. Chougale, A. B. Vantamuri and D. Kasai, Development and evaluation of Moringa extract incorporated Chitosan/Guar gum/Poly

(vinyl alcohol) active films for food packaging applications, *Int. J. Biol. Macromol.*, 2022, **200**, 50–60.
39 Z. S. Pour, P. Makvandi and M. Ghaemy, Performance properties and antibacterial activity of crosslinked films of quaternary ammonium modified starch and poly (vinyl alcohol), *Int. J. Biol. Macromol.*, 2015, **80**, 596–604.
40 A. Singh, B. Gaud and S. Jaybhaye, Optimization of synthesis parameters of silver nanoparticles and its antimicrobial activity, *Mater. Sci. Energy Technol.*, 2020, **3**, 232–236.
41 S. Roy, J.-W. Rhim and L. Jaiswal, Bioactive agar-based functional composite film incorporated with copper sulfide nanoparticles, *Food Hydrocolloids*, 2019, **93**, 156–166.
42 M. Kaya, S. Khadem, Y. S. Cakmak, M. Mujtaba, S. Ilk, L. Akyuz, A. M. Salaberria, J. Labidi, A. H. Abdulqadir and E. eligöz, Antioxidative and antimicrobial edible chitosan films blended with stem, leaf and seed extracts of Pistacia terebinthus for active food packaging, *RSC Adv.*, 2018, **8**(8), 3941–3950.
43 R. A. Hamouda, M. H. Hussein, R. A. Abo-Elmagd and S. S. Bawazir, Synthesis and biological characterization of silver nanoparticles derived from the cyanobacterium Oscillatoria limnetica, *Sci. Rep.*, 2019, **9**(1), 13071.
44 T. Gasti, V. D. Hiremani, S. S. Kesti, V. N. Vanjeri, N. Goudar, S. P. Masti, S. C. Thimmappa and R. B. Chougale, Physicochemical and Antibacterial Evaluation of Poly (Vinyl Alcohol)/Guar Gum/Silver Nanocomposite Films for Food Packaging Applications, *J. Polym. Environ.*, 2021, 1–17.
45 M. S. Sarwar, M. B. K. Niazi, Z. Jahan, T. Ahmad and A. Hussain, Preparation and characterization of PVA/nanocellulose/Ag nanocomposite films for antimicrobial food packaging, *Carbohydr. Polym.*, 2018, **184**, 453–464.
46 R. E. Ravindran, V. Subha and R. Ilangovan, Silver nanoparticles blended PEG/PVA nanocomposites synthesis and characterization for food packaging, *Arab. J. Chem.*, 2020, **13**(7), 6056–6060.
47 S. Hajji, H. Kchaou, I. Bkhairia, R. B. S.-B. Salem, S. Boufi, F. Debeaufort and M. Nasri, Conception of active food packaging films based on crab chitosan and gelatin enriched with crustacean protein hydrolysates with improved functional and biological properties, *Food Hydrocolloids*, 2021, **116**, 106639.
48 V. K. Pandey, S. N. Upadhyay, K. Niranjan and P. K. Mishra, Antimicrobial biodegradable chitosan-based composite Nano-layers for food packaging, *Int. J. Biol. Macromol.*, 2020, **157**, 212–219.
49 D. Liang, Z. Lu, H. Yang, J. Gao and R. Chen, Novel asymmetric wettable AgNPs/chitosan wound dressing: in vitro and in vivo evaluation, *ACS Appl. Mater. Interfaces*, 2016, **8**(6), 3958–3968.
50 S. Mathew, A. Jayakumar, V. P. Kumar, J. Mathew and E. K. Radhakrishnan, One-step synthesis of eco-friendly boiled rice starch blended polyvinyl alcohol bionanocomposite films decorated with in situ generated silver nanoparticles for food packaging purpose, *Int. J. Biol. Macromol.*, 2019, **139**, 475–485.
51 E. G. Lemraski, S. Yari, E. K. Ali, S. Sharafinia, H. Jahangirian, R. Rafiee-Moghaddam and T. J. Webster, Polyvinyl alcohol/chitosan/silver nanofibers as antibacterial agents and as efficient adsorbents to remove methyl orange from aqueous solutions, *J. Iran. Chem. Soc.*, 2022, **19**(4), 1287–1299.
52 V. G. Bhat, S. S. Narasagoudr, S. P. Masti, R. B. Chougale and Y. Shanbhag, Hydroxy citric acid cross-linked chitosan/guar gum/poly (vinyl alcohol) active films for food packaging applications, *Int. J. Biol. Macromol.*, 2021, **177**, 166–175.
53 V. G. Bhat, S. P. Masti, S. S. Narasagoudr, R. B. Chougale, P. K. SK and A. B. Vantamuri, Development and characterization of Chitosan/Guar gum/Gum ghatti bionanocomposites with in situ silver nanoparticles, *Chem. Data Collect.*, 2023, **44**, 101009.
54 A. M. Mostafa and A. Menazea, Polyvinyl Alcohol/Silver nanoparticles film prepared via pulsed laser ablation: An eco-friendly nano-catalyst for 4-nitrophenol degradation, *J. Mol. Struct.*, 2020, **1212**, 128125.
55 L. Y. Jun, N. Mubarak, L. S. Yon, C. H. Bing, M. Khalid, P. Jagadish and E. Abdullah, Immobilization of peroxidase on functionalized MWCNTs-buckypaper/polyvinyl alcohol nanocomposite membrane, *Sci. Rep.*, 2019, **9**(1), 2215.
56 M. Azizi, S. Sedaghat, K. Tahvildari, P. Derakhshi and A. Ghaemi, Green biosynthesis of silver nanoparticles with Eryngium caucasicum Trautv aqueous extract, *Inorg. Nano-Met. Chem.*, 2020, **50**(6), 429–436.
57 M. Cobos, I. De-La-Pinta, G. Quindós, M. J. Fernández and M. D. Fernández, One-step eco-friendly synthesized silver-graphene oxide/poly (vinyl alcohol) antibacterial nanocomposites, *Carbon*, 2019, **150**, 101–116.
58 C. B. Hiragond, A. S. Kshirsagar, V. V. Dhapte, T. Khanna, P. Joshi and P. V. More, Enhanced anti-microbial response of commercial face mask using colloidal silver nanoparticles, *Vacuum*, 2018, **156**, 475–482.
59 Y. Htwe, W. Chow, Y. Suda and M. Mariatti, Effect of silver nitrate concentration on the production of silver nanoparticles by green method, *Mater. Today: Proc.*, 2019, **17**, 568–573.
60 K. B. Narayanan and S. S. Han, Dual-crosslinked poly (vinyl alcohol)/sodium alginate/silver nanocomposite beads–A promising antimicrobial material, *Food Chem.*, 2017, **234**, 103–110.
61 O. F. Nwabor, S. Singh, S. Paosen, K. Vongkamjan and S. P. Voravuthikunchai, Enhancement of food shelf life with polyvinyl alcohol-chitosan nanocomposite films from bioactive Eucalyptus leaf extracts, *Food Biosci.*, 2020, **36**, 100609.
62 N. Eghbalifam, M. Frounchi and S. Dadbin, Antibacterial silver nanoparticles in polyvinyl alcohol/sodium alginate blend produced by gamma irradiation, *Int. J. Biol. Macromol.*, 2015, **80**, 170–176.
63 S. A. Zahra, Y. N. Butt, S. Nasar, S. Akram, Q. Fatima and J. Ikram, Food packaging in perspective of microbial activity: a review, *J. microbiol., biotechnol. food sci.*, 2016, **6**(2), 752.
64 D. Moreira, B. Gullón, P. Gullón, A. Gomes and F. Tavaria, Bioactive packaging using antioxidant extracts for the

prevention of microbial food-spoilage, *Funct. Foods Nutraceuticals*, 2016, **7**(7), 3273–3282.

65 S. S. Narasagoudr, V. G. Hegde, R. B. Chougale, S. P. Masti, S. Vootla and R. B. Malabadi, Physico-chemical and functional properties of rutin induced chitosan/poly (vinyl alcohol) bioactive films for food packaging applications, *Food Hydrocolloids*, 2020, **109**, 106096.

66 A. Ounkaew, P. Kasemsiri, K. Jetsrisuparb, H. Uyama, Y.-I. Hsu, T. Boonmars, A. Artchayasawat, J. T. Knijnenburg and P. Chindaprasirt, Synthesis of nanocomposite hydrogel based carboxymethyl starch/polyvinyl alcohol/nanosilver for biomedical materials, *Carbohydr. Polym.*, 2020, **248**, 116767.

67 S. Birania, S. Kumar, N. Kumar, A. K. Attkan, A. Panghal, P. Rohilla and R. Kumar, Advances in development of biodegradable food packaging material from agricultural and agro-industry waste, *J. Food Process. Eng.*, 2022, **45**(1), e13930.

68 H. Cheng, L. Chen, D. J. McClements, T. Yang, Z. Zhang, F. Ren, M. Miao, Y. Tian and Z. Jin, Starch-based biodegradable packaging materials: A review of their preparation, characterization and diverse applications in the food industry, *Trends Food Sci. Technol.*, 2021, **114**, 70–82.

69 S. Mathew, S. Snigdha, J. Mathew and E. Radhakrishnan, Biodegradable and active nanocomposite pouches reinforced with silver nanoparticles for improved packaging of chicken sausages, *Food Packag. Shelf Life*, 2019, **19**, 155–166.

70 V. G. Bhat, S. P. Masti, S. S. Narasagoudr, R. B. Chougale, P. Kumar and A. B. Vantamuri, Development and characterization of Chitosan/Guar gum/Gum ghatti bionanocomposites with in situ silver nanoparticles, *Chem. Data Collect.*, 2023, **44**(2405–8300), 101009.

71 T. Gasti, *et al.*, Physicochemical and Antibacterial Evaluation of Poly (Vinyl Alcohol)/Guar Gum/Silver Nanocomposite Films for Food Packaging Applications, *J. Polym. Environ.*, 2021, **29**(10), 3347–3363, DOI: 10.1007/s10924-021-02123-4.

72 N. Pal, M. Agarwal and A. Ghosh, Green synthesis of silver nanoparticles using polysaccharide-based guar gum, *Mater. Today Proc.*, 2023, **76**, 212–218, DOI: 10.1016/j.matpr.2023.01.048.

73 M. N. Gunaki, S. P. Masti, L. K. Kurabetta, J. P. Pinto, A. A. Hunashyal, R. B. Chougale and P. K. SK, Influence of chitosan-capped quercetin nanoparticles on chitosan/poly (vinyl) alcohol multifunctional films: A sustainable approach for bread preservation, *Int. J. Biol. Macromol.*, 2025, **299**, 140029.

74 L. K. Kurabetta, S. P. Masti, M. N. Gunaki, A. A. Hunashyal, R. B. Chougale, N. P. Dalbanjan and P. K. SK, Vanillin reinforced cationic starch/poly (vinyl alcohol) based antimicrobial and antioxidant bioactive films: sustainable food packaging materials, *Sustain. Food Technol.*, 2025, **3**, 1353–1364.

75 J. P. Pinto, M. H. Anandalli, A. A. Hunashyal, Priyadarshini and S. P. Masti, Carbon nanotubes reinforced chitosan/poly (1-vinylpyrrolidone-co-vinyl acetate) films: a sustainable approach for optoelectronic applications, *J. Mater. Sci.: Mater. Electron.*, 2025, **36**, 1035.

76 J. P. Pinto, V. D. Hiremani, O. J. D'souza, S. Khanapure, S. S. Narasagoudr, S. P. Masti and R. B. Chougale, Development of Chitosan-Copovidone nanocomposite films with antioxidant and antibacterial properties for food packaging applications, *Food Human.*, 2023, **1**, 378–390.

77 L. K. Kurabetta, S. P. Masti, M. N. Gunaki, A. A. Hunashyal, M. P. Eelager, R. B. Chougale, P. K. SK and A. J. Kadapure, A synergistic influence of gallic acid/ZnO NPs to strengthen the multifunctional properties of methylcellulose: A conservative approach for tomato preservation, *Int. J. Biol. Macromol.*, 2024, **277**, 134191.

78 L. K. Kurabetta, S. P. Masti, M. N. Gunaki, A. A. Hunashyal, R. B. Chougale, P. K. SK and A. J. Kadapure, Exploration of physicochemical and biological properties of phenylalanine incorporated carboxymethyl cellulose/poly (vinyl alcohol) based bioactive films for food packaging application, *Food Biosci.*, 2024, **61**, 104869.

79 L. K. Kurabetta, S. P. Masti, M. P. Eelager, M. N. Gunaki, S. Madihalli, A. A. Hunashyal, R. B. Chougale, P. K. SK and A. J. Kadapure, Physicochemical and antioxidant properties of tannic acid crosslinked cationic starch/chitosan based active films for ladyfinger packaging application, *Int. J. Biol. Macromol.*, 2023, **253**, 127552.

80 A. A. Hunashyal, S. P. Masti, L. K. Kurabetta, M. N. Gunaki, S. Madihalli, J. P. Pinto, M. B. Megalamani, B. Thokchom, R. B. Yarajarla and R. B. Chougale, Neem leaf-derived carbon dot-embedded chitosan-based active films: a sustainable approach to prolong the shelf life of prawns, *Sustain. Food Technol.*, 2025, **3**, 2088–2107.

81 A. A. Hunashyal, S. P. Masti, M. P. Eelager, O. J. D'souza, L. K. Kurabetta, R. B. Chougale and P. K. SK, Synergistic effects of Lantana camara leaf extract and in-situ AgNPs in chitosan/PVA films for lamb meat preservation, *Next Nanotechnol.*, 2025, **8**, 100292.

82 M. P. Eelager, S. P. Masti, S. Madihalli, N. Gouda, L. K. Kurbetta, M. N. Gunaki, R. B. Chougale and P. K. SK, The effect of cetrimide crosslinking on biodegradable PVA/xanthan gum herbicidal films: Towards sustainable agriculture and its influence on soil fertility, *J. Environ. Chem. Eng.*, 2025, **13**, 116029.

83 M. N. Gunaki, S. P. Masti, O. J. D'souza, M. P. Eelager, L. K. Kurabetta, R. B. Chougale, P. K. SK and A. J. Kadapure, Fabrication of CuO nanoparticles embedded novel chitosan/hydroxypropyl cellulose bio-nanocomposites for active packaging of jamun fruit, *Food Hydrocolloids*, 2024, **152**, 109937.

84 S. Madihalli, S. P. Masti, M. P. Eelager, R. B. Chougale, L. K. Kurabetta, A. A. Hunashyal, N. P. Dalbanjan and P. K. SK, Quinic acid and montmorillonite integrated chitosan/pullulan active films with potent antimicrobial and barrier properties to prolong the shelf life of tofu, *Food Biosci.*, 2024, **62**, 105492.

85 M. P. Eelager, S. P. Masti, N. P. Dalbanjan, S. Madihalli, M. N. Gunaki, L. K. Kurbetta, P. K. SK and R. B. Chougale, Atrazine integrated biodegradable poly (vinyl alcohol)/

xanthan gum active films for mulching applications: An alternative to microplastic generation plastic mulch, *Prog. Org. Coat.*, 2024, **192**, 108510.

86 M. N. Gunaki, S. P. Masti, L. K. Kurabetta, S. Madihalli, A. A. Hunashyal, R. B. Chougale, P. K. SK and A. J. Kadapure, Chitosan-encapsulated CuO nanoparticles reinforced multifunctional chitosan/gelatine nanocomposite films: A promising extension of cherry and grape shelf life, *J. Environ. Chem. Eng.*, 2025, **13**, 118397.

87 J. P. Pinto, *et al.*, Sustained drug delivery of the β-blocker acebutolol hydrochloride *via* chitosan–bilimbi leaf extract films, *RSC Pharm.*, 2026, **3**(1), 150–167, DOI: 10.1039/D5PM00172B.

88 B. A. Sheeparamatti, *et al.*, Fabrication of gallic acid crosslinked chitosan/poly(1-vinylpyrrolidone- *co* -vinyl acetate) antioxidant films for green chilli packaging, *RSC Appl. Polym.*, 2026, **4**(2), 767–784.

89 A. A. Hunashyal, *et al.*, Sustainable biopolymeric films of gelatin/kappa-carrageenan reinforced with jackfruit-derived cellulose nanocrystals for mushroom packaging, *Sustain. Food Technol.*, 2026, DOI: 10.1039/D5FB00817D.